Seasonal effect on the accuracy of Land use/Land cover classification in the Bilate Sub-basin, Abaya-Chamo Basin, Rift valley Lakes Basin of Ethiopia.

Alemeshet Kebede Yimer[1], Alemseged Tamiru Haile[2], Samuel Dagalo Hatiye[3], Assefa Gedle Azeref[4]

[1]*Arba Minch Water Technology Institute, Faculty of Water Resource and Irrigation Engineering, Arba Minch University, Ethiopia. Email: alemekebe@yahoo.com/alemeshet.kebede@amu.edu.et*

[2]*International Water Management Institute, IWMI, Ethiopia. Email:a.t.haile@cgiar.org/alemsegedtamiru@yahoo.com*

[3]*Arba Minch Water Technology Institute, Water Resources Research Center; Faculty of Water Resource and Irrigation Engineering, Arba Minch University, Ethiopia. Email: samueldagalo@gmail.com*

[4]*Arba Minch Water Technology Institute, Faculty of Hydraulics and Water Resource Engineering, Arba Minch University, Ethiopia. Email: asefa.gedle@yahoo.com*

ABSTRACT

A correct and timely land use/land cover (LULC) classification provides indispensable information for the effective management of environmental and natural resources. However, earlier studies mapped the LULC map of Bilate Sub-basin using remote sensing images that were acquired for a single season. Hence, these studies did not consider the seasonal effects on the accuracy of LULC classification. Therefore, the objective of this study was to evaluate changes in classification accuracy for images acquired during wet and dry seasons in the Bilate Sub-basin. LULC of the study area was classified using the Landsat 8 satellite imageries. Based on field observations, we classified the LULC of the study area into 9 dominant classes. The classification for the two seasons resulted in a noticeable difference between the LULC composition of the study area because of seasonal differences in the classification accuracy. The overall accuracy of the LULC maps was 80%for the wet season and 90% for the dry season with Kappa coefficient values of 0.8 and 0.9 respectively. Therefore, the two seasons showed a significant difference in the overall accuracy of the classification. However, we discovered that when the classification accuracy was tested locally, that is for individual pixels, the results were not the same. In Bilate Sub-basin, several pixels (14.71%) were assigned to different LULC classes on the two seasons maps while 85.29% of the LULC classes remained unaltered in the two maps. According to the classification results, the season had a noticeable effect on the accuracy of LULC classification. This suggests that for LULC classification, multi-temporal images should be used rather than a single remote sensing image.

Keywords: : Bilate, classification accuracy, Image classification, LULC, multi-temporal analysis, remote sensing.

Received: 8 July,, 2020; Accepted in revised form November 12, 2020; Published: December, 2020

1. INTRODUCTION

A correct and timely land use/land cover (LULC) classification provides indispensable information for the effective management of environmental and natural resources. The accuracy of LULC mapping is strongly reliant on the quality of the input information. The main inputs for LULC classification include freely accessible Landsat 8 satellite image and Ground Control Points (GCPs). The presence of clouds, rainy weather, shadows, and illumination in images can cause difficulties for remote sensing applications of LULC classification accuracy (Hereher *et al*., 2012), and change detection (Mas and González, 2015). In areas where rainfed crop production is dominant, cultivated land can be classified as bare land in the dry season. Grassland may also appear as bare land in the dry season. Such problems can be overcome by using multi-seasonal data instead of single-season data for LULC mapping (Heinl and Tappeiner 2012; Clark 2017). However, most studies prepare LULC maps using images that are acquired in single-season (Priyakant *et al.*, 2012).

The reported accuracy of LULC classification in the literature usually ranges from 50 to 95% (Yu *et al.*, 2006; Castillejo-González *et al*., 2009 and Myint *et al*., 2011). Increased accuracy can be achieved by improving the quality of the reference data (i.e. GCPs). For instance, Platt and Rapoza (2008) improved the overall classification accuracy from 64% to 78% by using expert- based knowledge. Several other studies also indicated that the classification accuracy could be improved by the proper size of the training dataset (Zhuang *et al.,* 1994; Foody & Arora, 1997; Foody & Mathur, 2004a;) and using the best classification algorithm (Castillejo-González *et al.,* 2009). Researchers also demonstrated that the classification errors could be reduced using all-weather, day-and-night imaging, as well as canopy penetration and high spatial resolution digital airborne imagery (Yu *et al.*, 2006).

Classification accuracy shows temporal variation because of seasonal variations in spectral characteristics of different LULC classes (Schriever and Congalton, 1995). Hence, minimizing classification errors because of these seasonal effects was central for generating precise LULC maps. However, earlier studies used images for the single date (mostly in the dry season) which were arbitrarily selected for LULC classification (Priyakant *et al*., 2012). Rodriguez-Galiano *et al*. (2012) revealed that the classification of seasonal features such as crops could be highly accurate if the information was extracted from multi-seasonal instead of mono-seasonal satellite images. Similarly, Löw *et al.* (2013) reported an increase in classification accuracy by up to 4.3% as a result of using the

most important features from multi-season images. Several studies were published on LULC classification in many parts of Ethiopia (Wagesho & Goel, 2013; Estifanos and Gebremariam, 2019; Degife *et al.*, 2019; Dibaba *et al*., 2020). However, these earlier studies used mono-season images for the classification (Estifanos and Gebremariam, 2019; Dibaba *et al.*, 2020) while ignoring the seasonal effects on spectral responses of LULC features. As a result, the studies reported overall classification accuracy of less than 85% (Yan *et al*., 2006; Platt and Rapoza, 2008) and did not attempt to improve the accuracy using multi-season (multi-temporal) information from satellite images. This limitation was also observed in Wagesho & Goel (2013) and (Sendabo, 2007) whose studies focused on Bilate Sub-basin.

In this study, the Landsat-8 imageries acquired in the dry and wet seasons were used to evaluate the classification errors because of seasonal differences in spectral responses. The findings of this study will contribute to measuring the magnitude of the existing LULC classification and it is a critical step that should be considered in the environmental protection strategy and sustainable resource management of basins. For the Bilate Sub-basin, such study is crucial and urgent considering the increasing and alarming intensity of anthropogenic activities in the landscape, and the need for implementing environmental protection policies in the basin. Therefore, the overall objectives of this study were to map the recent LULC and examine the impact of seasonality on the classification accuracy in Bilate Sub-basin, Abaya-Chamo Basin, Rift Valley Basin of Ethiopia.

2. STUDY AREA AND DATA SETS

2.1 Description of the study area

The Bilate Sub-basin lies between $37^0$47’14’’ to $38^0$20’14’’ E Longitude and $6^0$33’18’’ to $8^0$6’57’’N Latitudes. Bilate is among the major catchments of the Abaya-Chamo Sub-basin, which is part of the Rift Valley Lakes Basin. Guracha River, Guder River, and Weira River are tributaries of the Bilate River. These rivers join after passing the swampy Boyo Lake and named as Bilate River which drains to Lake Abaya. The Bilate Sub-basin covers an area of about 5330 km^2 at the gauging station at Bilate Tena with an elongated shape that stretches in the north-south direction (Wagesho & Goel, 2013). The altitude in the sub-basin ranges from 1,170 m.a.s.l. in the southern part up to 3,285 m.a.s.l. in the north.

Humid and semi-arid climatic conditions characterize the Bilate Sub-basin. It has a bimodal rainfall pattern with major rainfall during the summer monsoon season. The average annual rainfall variability is linearly correlated to the altitude in the catchment (Wagesho & Goel, 2013). Expansion of agricultural lands, cattle grazing, and timbering substantially reduced the vegetation cover in the watershed (Wagesho & Goel, 2013).

Deep gullies and massive bare soil at the upstream part of Bilate River Watershed shows its vulnerability to erosion hazard. The entire watershed practices a mixed cropping pattern where the middle and the lower watershed utilizes irrigation to grow commercial crops such as tobacco and maize (Wagesho, 2014). Currently, the demand for irrigation water is increasing and small-scale communal and medium-scale private investors are under the urgent course of water demand (Wagesho, 2014).

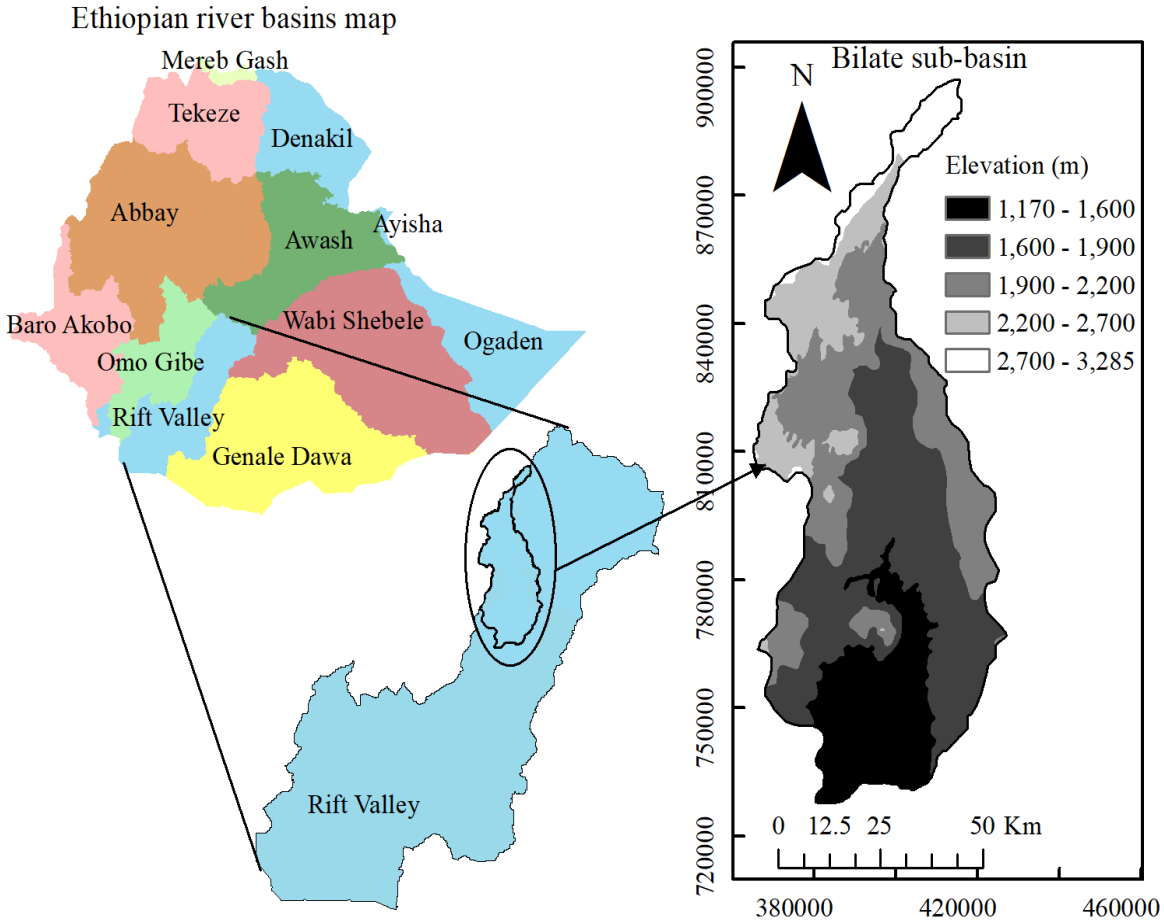

Figure 1. Location and elevation map of the Bilate sub-basin

2.2 Data Sets

In this study, both primary and secondary data were used. The primary data was collected by (i) a reconnaissance survey to identify key features of the catchment including the existing irrigated area, and (ii) an extensive field survey for the collection of Ground Control Points (GCPs) for image classification and geo-referencing. To better understand the temporal variations of LULC, local residents were surveyed.

The secondary data includes the Landsat 8 satellite imageries of 05-May-2018 and 12-May-2018 and 07-January-2019 and 16-January-2019 which were downloaded from the earth explorer data repository of the United States Geological Survey (USGS). As shown in Table1, three Landsat 8 spectral bands (bands 4,3, and2) were layer stacked to form one complete image with all bands to aid the interpreter in understanding all features in the study field.

Table 1. Description of the Landsat 8 images used in this study

Acquisition Date	Path/Row	Season	Spatial resolution(m)	Bands used (true colors)
05-May-18	168/055	Wet	30	4,3, and 2
05-May-18	168/056			
12-May-18	169/054			
12-May-18	169/055			
16-Jan-19	168/055	Dry	30	4,3, and 2
16-Jan-19	168/056			
07-Jan-19	169/054			
07-Jan-19	169/055			

3. MATERIALS AND METHODS

3.1 Mapping LU/LC

The Landsat 8 imageries of May-2018 and January-2019 were processed using ArcMap 10.3. Since Bilate Sub-basin covers a large area, four scenes of Landsat were mosaiced for both seasons.

The state of the atmosphere affects the qualities of images conspicuously, practically in the visible bands. Thus, removing the atmospheric effects has become a key step to improve the qualities of the images and to retrieve the actual reflectivity of surface features. First, the digital numbers (DN) are converted into the meaningful top of atmosphere (TOA) reflectance.

Next TOA reflectance was converted into surface reflectance by undertaking atmospheric correction. Also, georeferencing was done using 12 GCPs that were taken at road junctions, the bridge, and distinct river bends. These GCPs are fairly distributed over the upper, lower, and middle parts of the catchment. It is highly recommended to use an average root mean squared error (RMSE) value below 1.0 pixel as a target to accept the results of the georeferencing (Yesuf *et al*., 2015). We were able to attain this target by using only nine of the twelve GCPs. All the maps were projected to a Universal Transverse Mercator (UTM) coordinate system, Datum WGS 1984, zone 37 North of the study area.

In this study, the Maximum Likelihood (ML) algorithm was used for the supervised classification of the multi-temporal images. ML is a widely accepted classification method because of its robustness and simplicity for LULC classification (Lillesand and Kiefer, 2000; Degife *et al*., 2019; Dibaba *et al.*, 2020). The classifier determines the probability that a pixel belongs to each class and then assigns the pixel to the class with the highest probability (Richards and Jia, 1999).

Field observation was carried out based on checklists designed in advance to collect GCPs for the LULC in the sub-basin. With the aid of field observation, nine major LULC units were identified for the study area Bilate Sub-basin as shown in Table 2.

Table 2. LULC types in Bilate Sub-basin and their descriptions, classification system description (adapted and modified from Kebede (2009); Mengistu (2009); Gedle (2018))

Land Cover	Sub – category and description		Ground control points (GCPs)
	Sub – category	Description	
Forest	✓ Dense forest (70-100%) Individual plants are overlapping or slightly separated or touched. ✓ Moderate forest (30-69%) Individual plants are clearly separated or rarely touching ✓ Sparse forest (<30%) Individual plants are well separated and it is dominated by other species like shrubs and grasses	✓ Thick vegetation stands of grooves of evergreen and deciduous trees forming a dense canopy. It is predominantly covered by a tree (>5m high) with a single stem or branches well above the base ✓ Deciduous forest land Areas having a predominance of tree that lose their leaves at the beginning of a dry season ✓ Evergreen forest land Trees which predominantly remain green throughout the year. ✓ Mixed Forest land Areas where both evergreen and deciduous trees are growing and neither predominating.	Moderate forest (Acacia)

Land Cover	Sub – category and description		Ground control points (GCPs)
	Sub – category	Description	
Agriculture	✓ This category includes areas for the production of adapted crops for harvest, both annuals and perennials, and the scattered rural settlements that are closely associated with the cultivated fields. ✓ It includes areas currently under crop, fallow and land under preparation. which are: Irrigated agriculture and Rain fed agriculture ✓ Annual crop land: - complete their life cycle in one season and then die. ✓ Perennial crop land: - Are crops that are alive year-round and are harvested multiple times before dying.		
	Rain-fed agriculture	✓ The Period from April to October ✓ Annual crop land Maize, Tobacco, Local and Sweet potato, Wheat, Beans, Cotton, Barely, Teff, Sorghum, oil seeds etc ✓ Perennial crop land Sugarcane, Banana, Coffee, Enset, Chat etc	Banana, Bean, Tobacco, Maize, Potato, Cotton, Chat, Teff, Wheat, Enset (False banana)
	Irrigated agriculture	✓ The Period from November to March ✓ Annual crop land Maize, Tobacco, Wheat, Beans, Cotton, onion, local and sweet potato, oil seeds etc ✓ perennial crop land Sugarcane, Banana, Coffee, Enset, Chat etc	Banana, Bean Tobacco, Maize, Potato, Cotton, Chat, Teff, Wheat, Enset (False banana)

Land Cover	Sub – category and description		Ground control points (GCPs
	Sub – category	Description	
Shrubs	Dense shrub	✓ Area covered by small trees, bushes, and shrubs mixed with grasses	Shrubs mixed with grasses
	Sparse/open shrubs	✓ Mixed with trees, mixed with grass, Mixed with a bare ground	Mixed with a scattered tree,
Grass	Grass land	✓ Open grass land, Closed grass land, mixed with a tree, Mixed with shrubs.	Mixed with shrub and tree, Open grass, Mixed with scattered tree
Eucalyptus	A Fast-growing evergreen tree native to Australia.		Moderate, Dense, Sparce
Settlement	Residential, Commercial and service, Industrial, Public administration, Buildings, Paved Roads		Asphalt, Building, Bridge
Water body	Inland water bodies, Inland running water (streams & water channels) Inland wetlands, wetlands		Stream, Lake, Pond
Cultivated land	That is a type of ground, land, soil not sawn for one or more growing seasons and it is land used for planting crops, usually land with fertile soil and access to sufficient water for irrigation.		Cultivated land
Other Land	Gravel Roads, Bare soils, Bare rocks Quarry, Gravel rocks		Bare rocks, Quarry, Local house, Bare soil

The quantity, distribution, and accuracy of GCPs play an important role in training image classification algorithms. In this, the number of sample points was calculated using the equation based on the binomial probability theory. The Cochran Model allows calculating an ideal sample size given a desired level of precision, desired confidence level, and the estimated proportion of the attribute present in the population (Congalton, 1991; Foody, 2006). The equation reads:

$$N = \frac{Z^2 pq}{E^2} \quad (1)$$

where: N is the sample size, E is the desired level of precision (i.e. the margin of error), p is the (estimated) proportion of the population that has the attribute in question, q is 1 – p, and Z is z-score. In this study, the minimum sampling size is estimated for Z=1.96, p=85%, q=15%, and E=4%. This resulted in a minimum sample size (N) =319 according to equation (1). Therefore, we decided to collect 470 GCPs for each season.

The traditional climate zone classification of Ethiopia is based on altitude and temperature. Based on such classification, there are five climate zones: Wurchi (cold climate at more than 3000m altitudes), Dega (temperate like climate-highland with 2500-3000m altitudes), Weynadega (Warm climate with 1500-2500m altitude), Kola (Hot and arid type with less than 1500m altitudes) and Bereha (hot and hyper-arid type) climate (NMA, 2001). According to this classification, the majority part of the study area falls under Weynadega and Kola (Figure 2) but there is also fairly large coverage of other zones. Thus, the GCPs were collected from each of the dominant climate zones of the study area (Figure 2) whereas their spatial distribution was mainly determined by site accessibility. We made sure that the sampled areas had a heterogeneous land cover so that they could represent the entire catchment. 470 GCPs were collected twice, i.e., for the wet season (May-2018) and dry season (January-2019).

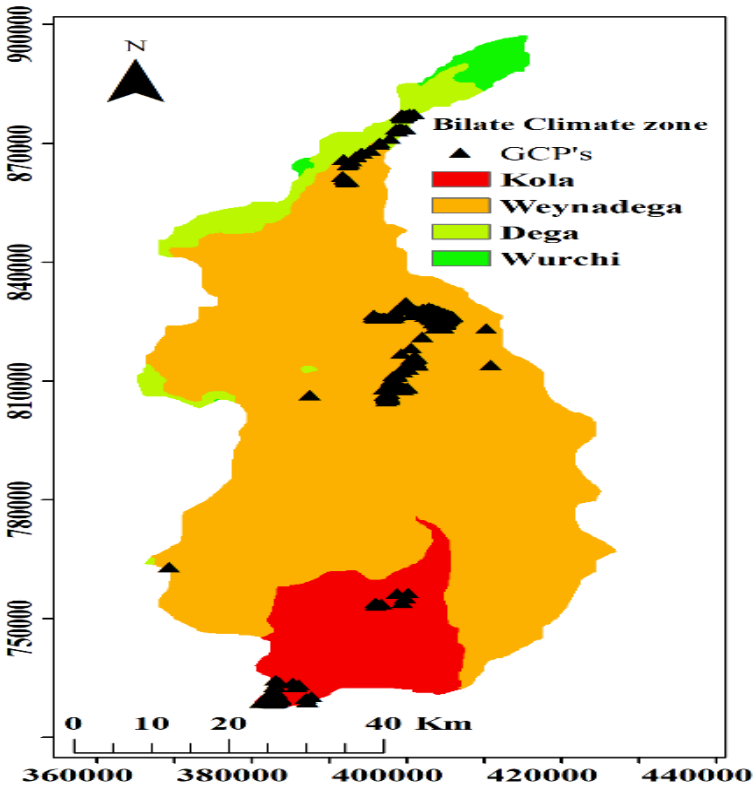

Figure 2**.** Distribution of the GCPs over the climate zones of Bilate Sub-basin.

Out of the total 470 GCPs, 80% (376 GCPs) were used for training the classification algorithm whereas 20 % (94 GCPs) were used for validation of the classified image.

3.2 Classification accuracy assessment

Accuracy assessment is an important step in remote sensing to verify the fitness of classification products. The most common way to assess the accuracy of a classified map is to create a set of random points from the ground truth data and compare that to the classified data in a confusion matrix. In this study, out of 470 GCP's 20 % (94 GCP's) were selected randomly to serve as reference (validation) data for the accuracy assessment. The confusion matrix is used to calculate the accuracy metrics, which are overall accuracy, omission, commission, and kappa coefficient.

The overall accuracy was calculated by summing the number of pixels classified correctly and dividing them by the total number of pixels. Thus, it showed what proportion of the reference sites (GCPs) were mapped correctly. The overall accuracy was usually expressed in percentages, with 100% accuracy being a perfect classification whereas >85% was considered as an acceptable level of accuracy (Gashaw

et al., 2017). The diagonal elements of the confusion matrix represented the pixels that were correctly classified.

The confusion matrix was also used to assess the accuracy of the user and that of the producer. The accuracy of the user refers to the probability that class I remains the same on the ground in a classified image (reference data). The use of values across rows for each class was estimated in the confusion matrix and the correct classifications were added together and divided by the total number of classified pixels for each class.

The accuracy of the producer was the likelihood that the class j in the classified image would be mapped on the ground (reference) as the same class. For each class, producer accuracy was determined by going down the columns and adding the correct classifications together, and dividing them by the total number of reference sites for each class.

Omission applies to the reference data left out (omitted) in the secret map of the correct class. For each class, Omission is determined by going down the columns and adding the wrong classification together, and dividing it by the total number of reference sites for each class.

The Commission refers to pixels listed as reference sites that have been left out of the classified class map. For each class, Commission is determined by passing through the rows and adding the wrong classification, and dividing it by the total number of classified places for each class.

We used the Kappa coefficient to evaluate the agreement between the classified map and the reality on the ground (Cohen, 1960).The Kappa coefficient of 0 indicated an absolute disagreement between the map and the truth, and 1 indicated complete agreement.

The equation for the Kappa coefficient (κ) reads as follows.

$$\kappa=\frac{P_o-P_c}{1-P_c} \qquad (2)$$

Where: $P_o=\sum P_{ii}$ is the sum of relative frequency in the diagonal of the actual error matrix, and $P_c=\sum P_{i+}P_{+j}$ is the relative frequency of a random allocation of observations to the cells chance agreement. The notations "i+" and "+*j*" stand for the relative marginal frequencies. When Kappa value is greater than 0.80, it shows a good classification performance; however, the values between 0.40 and 0.80

indicate moderate classification performance; and When the Kappa values fall below 0.40, it indicates poor classification performance (Lillesand *et al*., 2004; Jensen, 2005).

The analysis of the difference in the study area using ArcMap 10.3 resulted in a pixel over pixel-based classification comparison of Landsat 8, the wet season and dry season LULC classification image.

4. RESULTS AND DISCUSSION

4.1 Classification accuracy matrixes

Multi-temporal (wet and dry) season images were used to examine the impact of seasonality on the LULC classification accuracy. The average cloud coverage for wet season images is 16.5 percent and 0.78 percent for the dry season. Due to the reduced availability of cloud-free images in the rainy season compared to the dry season, all images for the wet season have been masked and atmospherically corrected. The data suggested that the classification results were more accurate during the dry season than the wet season. The highest classification accuracy was provided by a cloud-free image of January-2019, which referred to the dry season. In contrast, the image on May-2018, which stood for the wet season, showed the lowest accuracy.

Table 3 showed the classification accuracy of the LULC maps for the dry and wet seasons. The results of the dry season classification were better than the wet season in terms of overall accuracy and kappa coefficient measurements.

The overall accuracy was 80% for the wet season map and 90% for the dry season map. This indicated the presence of variations in classification accuracy with images taken in different seasons. The dry season map had a very good overall accuracy but the overall accuracy of the wet season map was not acceptable (<85%). This suggested that the map was unfit for other applications. This was supported by the values of the Kappa coefficient that indicated the reliability of the result. The Kappa coefficients were 0.8 and 0.9 for the dry and wet seasons, respectively (Lillesand *et al.,* 2004; Jensen, 2005).

Table 3. Accuracy assessments of LULC classes

Season	Land use class	Settlement	Waterbody	Perennial crops	Eucalyptus	Shrub	Cultivated land	Grass	Bare Land	Annual crops	Ground truth	**User accuracy**	**Kappa Coefficient**
wet season	Settlement	9	0	0	0	0	0	0	1	1	11	**75.0**	**0.8**
	Water body	1	14	0	0	0	0	0	0	0	15	**93.3**	
	Perennial crops	0	0	3	0	0	1	0	0	0	4	**75.0**	
	Eucalyptus	0	0	0	5	0	0	1	0	1	7	**83.3**	
	Shrub	0	0	0	0	9	0	2	0	1	12	**90.0**	
	Cultivated land	0	0	0	0	0	4	0	0	0	5	**66.7**	
	Grass	1	1	0	0	0	0	15	0	0	17	**83.3**	
	Bare Land	1	0	0	1	0	1	0	11	0	14	**84.6**	
	Annual crops	1	0	1	0	1	0	0	1	7	10	**70.0**	
	Total	13	15	4	6	10	6	18	13	10	95		
	Producers Accuracy	**81.8**	**93.3**	**75.0**	**71.4**	**75.0**	**80.0**	**88.2**	**78.6**	**70.0**			
	Overall accuracy						**0.8**						
Dry season	Settlement	10	0	0	0	0	0	0	1	1	12	**83.3**	**0.9**
	Water body	1	11	0	0	0	0	0	0	0	12	**91.7**	
	Perennial crops	0	0	4	0	0	0	0	0	0	4	**80.0**	
	Eucalyptus	0	0	0	5	0	0	0	0	1	6	**83.3**	
	Shrub	0	0	0	0	8	0	1	0	1	10	**88.9**	
	Cultivated land	0	0	0	0	0	5	0	0	0	5	**83.3**	
	Grass	1	1	0	0	0	0	14	0	0	16	**93.3**	
	Bare Land	0	0	0	1	0	1	0	16	0	18	**88.9**	
	Annual crops	0	0	1	0	1	0	0	1	8	11	**72.7**	
	Total	12	12	5	6	9	6	15	18	11	94		
	Producers Accuracy	**83.3**	**91.7**	**100.0**	**83.3**	**80.0**	**100.0**	**87.5**	**88.9**	**72.7**			
	Overall accuracy						**0.9**						

The availability of cloud-free images was limited in the wet season in comparison to the dry season. Table 4 showed that the classifications of dry season images produced the highest classification

accuracy whereas, the wet season image showed the lowest accuracy or produced higher errors (commission and omission).

The cultivated land in the wet season had a 20% commission error and 33.3% omission error (Table 4). However, during the dry season, cultivated land commission and omission errors decreased to 0.0 percent and 16.7 percent in January-2019. Again, the commission error in the dry season was significantly smaller than that of the wet season for perennial crops. According to the classification accuracy results, the season effect on the commission and omission errors was pronounced for all LULC classes.

Table 4. Accuracy assessments of LULC classes

LULC class	Wet season (May-2018)		Dry season (January-2019)	
	Commission	Omission	Commission	Omission
Settlement	18.18	25.0	16.67	16.7
Water body	6.67	6.7	8.33	8.3
Perennial crops	25.00	25.0	0.00	20.0
Eucalyptus	28.57	16.7	16.67	16.7
Shrub	25.00	10.0	20.00	11.1
Cultivated land	20.00	33.3	0.00	16.7
Grass	11.76	16.7	12.50	6.7
Bare land	21.43	15.4	11.11	11.1
Annual crops	30.00	30.0	27.27	27.3

4.2 LULC classification system

We prepared LULC maps of the dry and wet seasons for Bilate Sub-basin (Figure 3). In this study, the LULC classification was categorized into nine dominant LULC classes: settlement (SE), water body (WB), perennial crops (PC), eucalyptus (EU), shrub (SH), cultivated land (CL), grass (GR), bare land (BL) and annual crops (AC). Similar to the topographic and climatic variation in the Bilate Sub-basin, there was a distinct North to South and West to East gradient in the spatial variation of the LULC classes.

The cross-section from North to South showed that the Bilate Sub-basin was mostly in a steep slope almost up to the river's mouth. Besides, the cross-section from West to East showed the diversity of topography and steepness. Besides, the climatic condition showed variations depending on the agroecology and the altitude (Sendabo, 2007).

The purpose of this study was to map LULC and observe the effect of seasonality on classification accuracy. Therefore, the wet season map showed that: the northern part was dominantly covered by eucalyptus plantation, perennial crops, and grassland. In the middle part of the catchment, the eucalyptus tree was dominant over the western part whereas the eastern part was mostly covered with annual crops with some bare land and grassland. The most downstream (southern) part of the catchment was mostly grassland, annual crops cultivated land, and bare land.

Overall, it seemed that there was no significant difference between the two maps in terms of the spatial pattern of LULC classes. However, a closer inspection of the maps showed that there was some clear difference. Depending on the landscape and topography of the sub-basin over the northern part, eucalyptus trees and grassland were more prominent in the wet season than in the dry season map. During the rainy season, the annual crop was grown in the middle-eastern portion of the sub-basin. However, it was missing in the dry season map as expected.

This suggested that the dry season map underestimated the size of the cultivated land. There was also some difference between the two maps in the downstream part of the sub-basin. In the dry season, the image would be within the irrigation period (November to March). Because of the intensive irrigation, the field coverage of annual and perennial crops was greater in the dry season.

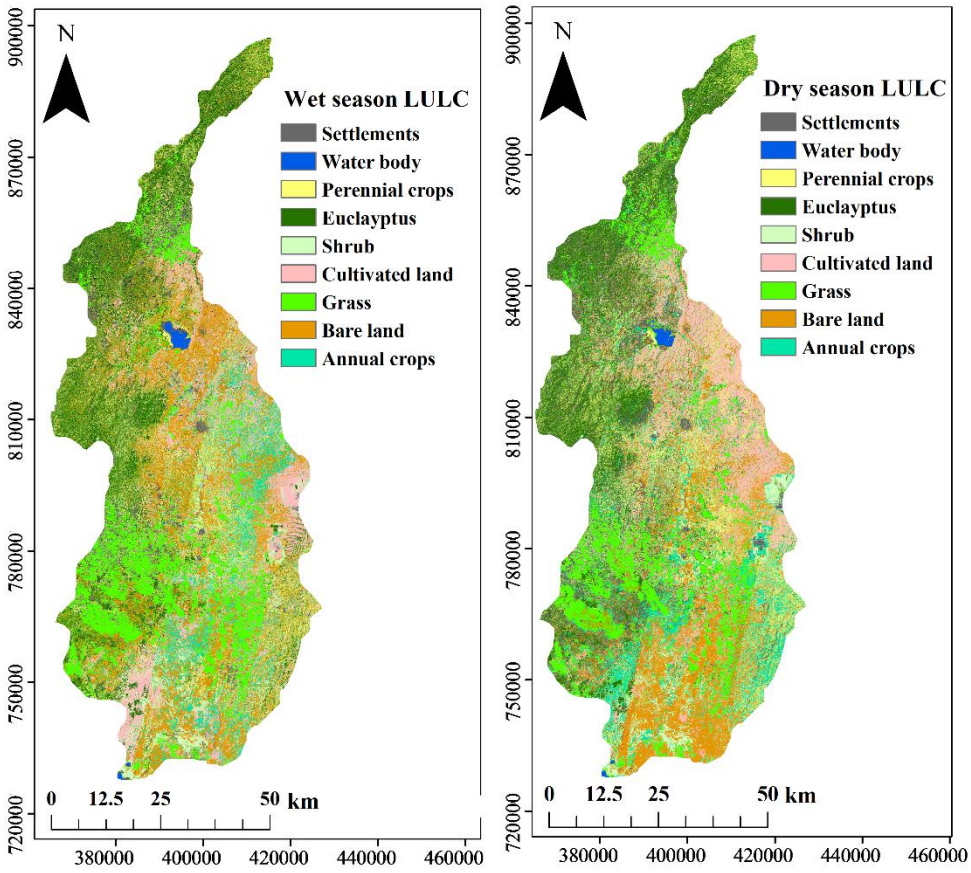

Figure 3. LULC maps based on classification of Landsat 8 images of May-2018 and January-2019.

The seasonal effect on the area covered by LULC class was evaluated by comparing the area extracted from the dry and wet season maps of the study area. The wet season map was considered the base map. The area difference in LULC change between the dry and wet season maps was shown in Table 5.

The highest percentage difference between the two maps was obtained from the water body and bare land. The water body was reduced by 35% and bare land was increased by 35% in the dry season map as compared to that on the wet season map. Except for the seasonal effect, the direction of these differences was predicted, but the magnitudes are enormous. In addition, the extent of grassland and annual crops varies greatly between the two maps. The extents of grassland and annual crops also show a significant difference in the two maps. The area of the settlement and perennial crops remained the same in the two maps. The eucalyptus cover decreased in the dry season. This could be attributed to either the classification error or people cutting the tree. Local residents were interviewed to gain a better understanding of the insignificant temporal variations in annual crops. They stated that farmers did not irrigate large areas in the dry season of 2019 because of fuel shortage for the water pump. Hence, the

difference in annual crop coverage was different in the two maps owing to classification error or decrease in irrigation as the cultivated area was classified as bare land in the dry season.

Table 5. Comparison of the area covered by each LULC class on the dry and wet season maps

LULC Area (km^2)			
LULC class	Wet season	Dry season	Difference (%)
Settlements	509.06	509.08	0.00
Water body	74.05	54.83	-35.05
Perennial crops	620.68	620.15	-0.09
Eucalyptus	1018.89	940.95	-8.28
Shrub	476.24	445.67	-6.86
Cultivated land	673.46	750.88	10.31
Grass	964.34	791.45	-21.84
Bare land	566.04	881.65	35.80
Annual crops	447.07	354.70	-26.04
Total	**5349.35**	**5349.35**	

4.3 Temporal analysis of LULC

Figure 4 showed the location of changed and unchanged areas, highlighted with different colors. Only changed areas were used to visualize the overall dynamics. Differences were observed between wet and dry seasons; significant losses were noticed in the grass, annual crop, eucalyptus, shrub, and water body, whereas gain was observed in bare land and cultivated land. Grassland, shrubs, annual crops, and water body at the middle, lower and upper parts of the Bilate Sub-basin were changed to cultivated and bare land in the dry season.

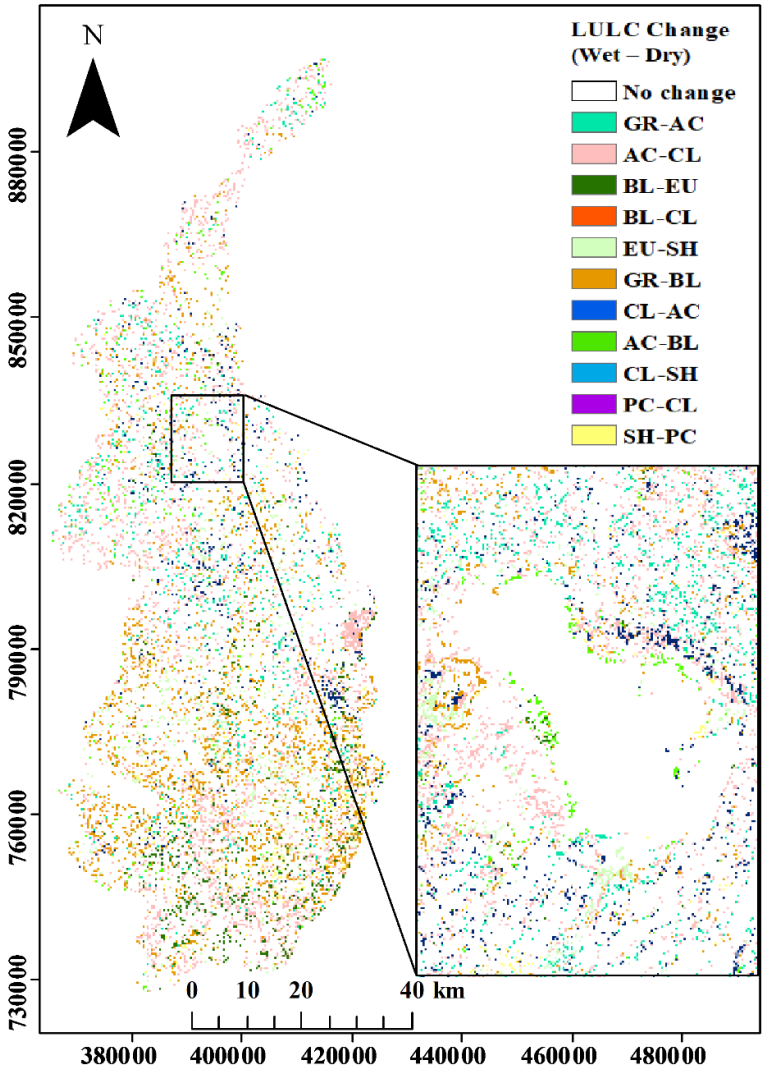

Figure 4. The difference in LULC in Bilate Sub-basin based on classification using images of dry and wet seasons.

Along with LULC differences, a land-use conversion matrix was used to depict which land use classes were converted very rapidly to other land uses (Table 6). In the matrix, the diagonal values represented the proportion of land use that remained unchanged during the wet-dry seasons. In Bilate Sub-basin, 14.71% of the total land area under different land-use categories were converted from one category of land use to another category while the remaining 85.29% was unaltered. Among various types of LULC classes, the grass was mostly converted to other land uses. In between the wet and dry seasons, about 5% of the area was converted from bare land to cultivated land, followed by 3.1% in the grass, 1.2% in the annual crop, and 2% in shrub areas.

Table 6. The LULC classes difference matrix from wet to dry season

		LULC dry season								
	LULC Class	**AC**	**BL**	**CL**	**EU**	**GR**	**PC**	**SE**	**SH**	**WB**
LULC wet season	**AC**	0.10	1.20	0.70	1.30	0.00	2.20	0.60	0.60	0.00
	BL	2.40	0.00	0.10	4.00	2.10	3.10	2.30	4.00	0.80
	CL	2.80	5.00	1.00	2.20	2.30	1.10	1.50	1.40	0.00
	EU	0.20	0.10	3.10	0.10	5.00	5.00	2.60	1.40	0.00
	GR	0.50	3.10	3.80	1.70	0.20	0.60	3.10	1.60	0.40
	PC	0.20	0.30	4.50	3.00	3.00	0.10	0.00	0.10	0.00
	SE	0.10	0.00	0.00	5.00	4.00	0.70	0.00	0.00	0.00
	SH	2.20	2.00	0.00	3.70	1.40	1.00	0.00	0.10	0.10
	WB	0.00	0.08	0.30	0.10	0.30	0.00	0.00	0.30	0.00
	From (%)	**8.36**	**10.58**	**12.59**	**19.05**	**18.03**	**11.60**	**9.52**	**8.90**	**1.38**
	To (%)	**6.63**	**16.48**	**14.04**	**17.59**	**14.80**	**11.59**	**9.52**	**8.33**	**1.03**

The Bilate Sub-basin is referred to the place where bare land and cultivated land area have increased and at the same time grass, eucalyptus, annual crop, perennial crop, water body, and shrub area decreased over the analysis periods. Substantial land use difference was observed in the bare land, grass, annual crop, and the cultivated land. This difference could be associated mostly with seasonal effects on classification accuracy.

To show clearly this difference, the overall change was presented for the wet and dry seasons (Table 7 and Figure 5). The existing forest and wetland cover of the Bilate Sub-basin was negligible as observed, as it was transformed to other forms of land cover.

Table 7. The LULC difference from wet to dry seasons

	Percentage		
LULC class	Wet season (%)	Dry season (%)	Difference (%)
Settlements	9.52	9.52	0.00
Water body	1.38	1.03	-0.36
Perennial crops	11.60	11.59	-0.01
Eucalyptus	19.05	17.59	-1.46
Shrub	8.90	8.33	-0.57
Cultivated land	12.59	14.04	1.45
Grass	18.03	14.80	-3.23
Bare land	10.58	16.48	5.90
Annual crops	8.36	6.63	-1.73
Total	**100**	**100**	

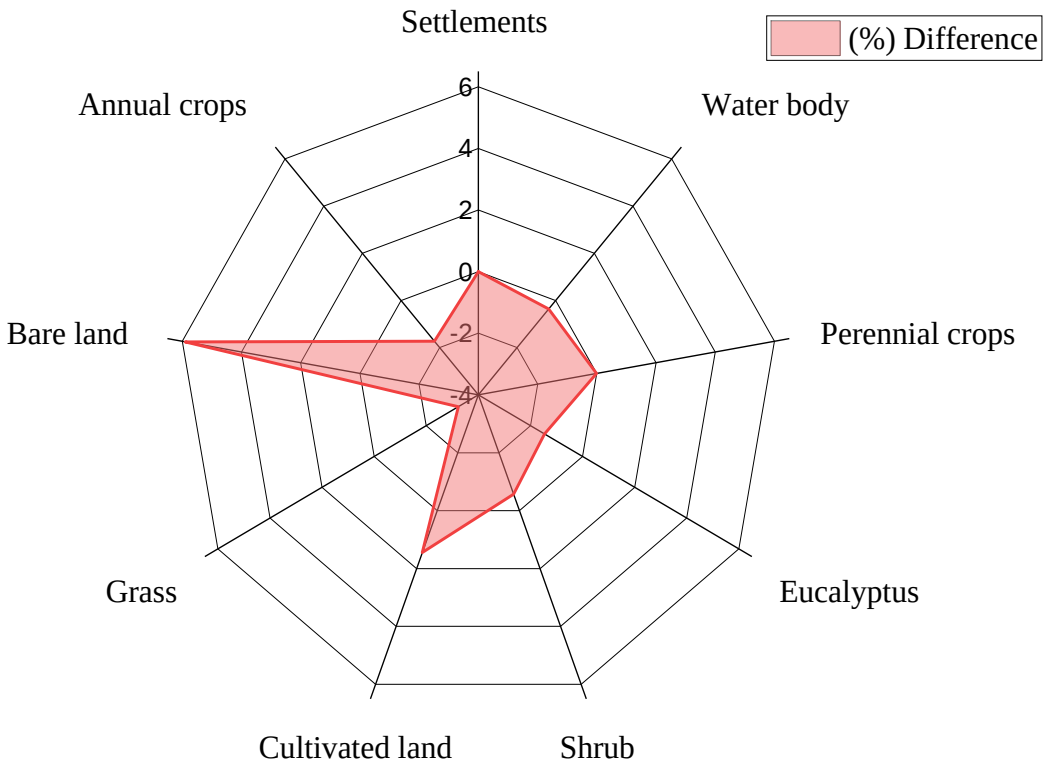

Figure 5. Percentage differences in LULC classes from wet to dry season

5. CONCLUSIONS

This study aimed at examining the impact of seasonality on the LULC classification accuracy in Bilate Sub-basin, Abaya-Chamo Basin, Rift Valley Basin of Ethiopia. The largest difference in percentage between the two season maps was obtained for the water body and bare land. The extents of grassland and annual crops also showed a significant difference in the two maps. However, the area of the settlement and perennial crops was not significantly changed by the seasonal effect on the classification. In this study multi-temporal (seasonal) LULC classification showed that the dry seasons map resulted in smaller area coverage of the grass, annual crop, eucalyptus, shrub, and water body than the wet season map. Grassland, shrubs, annual crops, and water body in the wet season map were changed to cultivated and bare land in the dry season map.

The accuracy assessment for the existing LULC classification was analyzed. According to the classification results, the overall accuracy was season-dependent. A higher overall classification was achieved for the dry season than the wet season map. Hence, the selection of a particular season could have a large impact on the accuracy and reliability of the resulting classification. Aside from the influence of the climate on classification accuracy, a particular region can be barren land one season and filled with crops the next. Similar seasonal variations might happen to other land cover classes including grassland and water bodies. This indicated the need for using multi-temporal images for LULC classification. Future studies can explore methods to produce single LULC maps based on the integration of information from multiple seasons.

REFERENCES

Ayele, G.T., Demessie S.S., Mengistu K.T., Tilahun S.A., and Melesse A.M. (2016). Multitemporal land use/land cover change detection for the Batena Watershed, Rift Valley Lakes Basin, Ethiopia. In Landscape dynamics, soils and hydrological processes in varied climates. Springer, Berlin, 51–72.

Castillejo-González, I. L., López-Granados. F., García-Ferrer, A., Peña-Barragán, J. M., Jurado Expósito, M., de la Orden, M. S. (2009). Object- and pixel-based analysis for mapping crops and their agro-environmental associated measures using Quick Bird imagery. Computers and Electronics in Agriculture. 68(2), 207–215.

Clark, M. L. (2017). Comparison of Simulated Hyperspectral HyspIRI and Multispectral Landsat 8 and Sentinel-2 Imagery for Multi-Seasonal, Regional Land-Cover Mapping. Remote Sensing of Environment 200, 311–325. DOI: 10.1016/j.rse.2017.08.028.

Clever, A., Ormad P., Rodríguez L., and Ovelleiro J.L. (2004). Study of the presence of pesticides in surface waters in the Ebro river basin (Spain). Chemosphere. 64, 1437–1443.

Cohen, J. (1960). A Coefficient of Agreement for nominal scales. Educational and Psychological Measurement. New York University. Vol. xx, No. 1.

Congalton, R. (1991). A review of assessing the accuracy of classification of remotely sensed data. Remote Sensing of Environment. 37, 35-46.

Congalton, R.G., and K. Green. (1999). Assessing the Accuracy of Remotely Sensed Data: Principle and Practices, Mapping Science Series, Lewis Publications, CRC Press.

Deblina, C., Kalikinkar D., Arijit D. (2017). Assessment of land use land cover changes and its impact on variations of land surface temperature in Asansol-Durgapur Development Region. The Egyptian Journal of Remote Sensing and Space Sciences. Department of Geography, University of Gour Banga, Mokdumpur, Malda Pin- 732103, India.

Degife, A., Worku, H., Gizaw, S., and Legessea, A. (2019). Land use land cover dynamics, its drivers and environmental implications in Lake Hawassa Watershed of Ethiopia. Remote Sensing Applications: Society and Environment. 14, 178–190.

Dibaba, W., T., Demissie, T., A., and Miegel, K. (2020). Drivers and Implications of Land Use/Land Cover Dynamics in Finchaa Catchment, Northwestern Ethiopia. Land 2020, 9, 113; doi:10.3390/land9040113

Estifanos, T., H., and Gebremariam, B. (2019). Modeling-impact of Land Use/Cover Change on Sediment Yield (Case Study on Omo-gibe Basin, Gilgel Gibe III Watershed, Ethiopia). American Journal of Modern Energy. 5 (6), 84-93. DOI: 10.11648/j.ajme.20190506.11

Fasona and Omojola. (2005). Land Use Conflict Between Farmers and Herdsmen – Implications for Agricultural and Rural Development in Nigeria. Rashid Solagberu Adisa Department of Agricultural Extension and Rural Development, University of Ilorin, Ilorin Nigeria.

Foody, G. M., & Arora, M. K. (1997). An evaluation of some factors affecting the accuracy of classification by an artificial neural network. International Journal of Remote Sensing. 18, 799−810.

Foody, G. M., & Mathur, A. (2004a). A relative evaluation of multiclass image classification by support vector machines. IEEE Transactions on Geoscience and Remote Sensing. pp42, 1335−1343.

Foody, G.M, Mathur, A., Hernandez, C.S, and Boyd, D.S. (2006). Training set size requirements for the classification of a specific class. Remote Sensing of Environment. 104, 1–14.

Gedle, A. (2018). The impact of land use-land cover changes on water availability in the kulfo watershed. M.Sc. Thesis work, Arba Minch University, Ethiopia. 91, 42-47.

Gupta, A. K. & Nair, S. S. (2010). Flood risk and context of land-uses: Chennai city case. J. Geographical Region Plan. 3, 365–372.

Halder, S., Saha, S. K., Dirmeyer, P. A., Chase, T. N. & Goswami, B. N. (2016). Investigating the impact of land-use land-cover change on Indian summer monsoon daily rainfall and temperature during 1951-2005 using a regional climate model. Hydrological Earth System. Sci. 20, 1765–1784.

Heinl, M., and U. Tappeiner. (2012). "The Benefits of considering Land Cover Seasonality in Multi-Spectral Image Classification." Journal of Land Use Science. 7 (1), 1–19. doi:10.1080/ 1747423X.2010.518168.

Hereher, M.E., Al-Shammari, A.M., Allah, S.E.A. (2012). Land cover classification of Hail-Saudi Arabia using remote sensing. Int. J. Geosci. 3, 349e356. https://doi.org/10.4236/ijg.2012.32038.

Jensen, J.R. (2005). Information extraction using artificial intelligence, In Introductory Digital Image Processing – A Remote Sensing Perspective, 3rd ed.; Editor, Keith, C.C., Ed.; Prentice-Hall Series in Geographic Information Science: Saddle River, NJ, USA, Sect. D. 407–429.

Kamh, S., Ashmawy, M., Kilias, A., & Christaras, B. (2012). Evaluating urban land cover change in the Hurghada area, Egypt, by using GIS and remote sensing. International Journal of Remote Sensing. 33(1), 41–68.

Kebede, E.W. (2009). Hydrological responses to land cover changes in Gilgel Abbay Catchment, Ethiopia. M.Sc. Thesis Work, ITC, Enschede.

Kumar, R. *et al.* (2017). Dominant control of agriculture and irrigation on urban heat island in India. Sci. Rep. 7, 1–10.

Liang, S., Fang H., Morisette J.T., Chen M, Shuey C.J., Walthall C.L., and Daughtry C.S. (2002). Atmospheric correction of Landsat ETM+ land surface imagery. II. Validation and applications. IEEE Trans Geosci Remote Sens. 40(12), 2736–2746.

Lillesand, T, M., Kiefer R. W., Chipman, J, W. (2004). Remote Sensing and Image Interpretation, Ed.5 John Wiley & Sons Ltd, ISBN 0471 30575.

Lillesand, T.M., and Kiefer, R.W. (2000). Remote Sensing and Image Interpretation, fourth ed. John Wiley & Sons, New York, NY, USA.

Lillesand, T.M., Kiefer, R.W., Chipman, J.W. (2008). Remote Sensing and Image Interpretation. John Wiley & Sons.

Liu, C., P. Frazier, and L. Kumar. (2007). Comparative assessment of the measures of thematic classification accuracy, Remote Sensing of Environment. 107, 606–616.

Löw, F., Michel, U., Dech, S., & Conrad, C. (2012). Impact of feature selection on the accuracy and spatial uncertainty of per-field crop classification using Support Vector Machines. ISPRS Journal of Photogrammetry and Remote Sensing. 85 (2013), 102–119

Mas, J. F. (2004). Mapping land use/cover in a tropical coastal area using satellite sensor data, GIS, and artificial neural networks. Estuarine, Coastal and Shelf Science. 59(2), 219–230.

Mas, J.F., González, R. (2015). Change detection and land use/land cover database updating using image segmentation, Gis analysis, and visual interpretation. ISPRS - Int. Arch. Photogramm. Remote Sens. Spat. Inf. Sci. 61e65. XL-3/W3. https://doi.org/10.5194/isprsarchives-XL-3-W3-61-2015.

Mengistu, K. T. (2009). Watershed Hydrological Responses to Changes in Land Use and Land Cover and Management Practices at Hare Watershed, Ethiopia. Hinweis zum Urheberrecht.

Dissertation zugänglich unter. URN: urn: nbn: de: hbz: 467-4201. URL: http://dokumentix.ub.uni-siegen.de/opus/volltexte/2009/420.

Mohan, M. & Kandya, A. (2015). Impact of urbanization and land-use/land-cover change on diurnal temperature range: A case study of tropical urban airshed of India using remote sensing data. Sci. Total Environ. 506–507, 453–465.

Muttitanon, W., & Tripathi, N. K. (2005). Land use/land cover changes in the coastal zone of Ban Don Bay, Thailand using Landsat 5TMdata. International Journal of Remote Sensing. 26(11), 2311–2323.

Myint, S. W., Gober, P., Brazel, A., Grossman-Clarke, S., & Weng, Q. (2011). Per-pixel vs. object-based classification of urban land cover extraction using high spatial resolution imagery. Remote Sensing of Environment. 115(5), 1145–1161.

Niyogi, D., Kishtawal, C., Tripathi, S. & Govindaraju, R.S. (2010). Observational evidence that agricultural intensification and land-use change may be reducing the Indian summer monsoon rainfall. Water Resour. Res. 46, 1–17.

NMA (National Meteorological Agency). (2001). Initial National Communication of Ethiopia to the United Nations Framework Convention on Climate Change (UNFCCC). National Meteorological Services Agency, Addis Ababa, Ethiopia. Addis Ababa. Ethiopia.

Ozdogan, M., and Yang Y., Allez G., and Cervantes, C. (2010). Remote sensing of irrigated agriculture: Opportunities and challenges. Remote Sensing. 2(9), 2274–2304.

Paul, S. *et al*. (2016). Weakening of Indian Summer Monsoon Rainfall due to Changes in Land Use Land Cover. Sci. Rep. 6, 1–10.

Platt, R. V., & Rapoza, L. (2008). An evaluation of an object-oriented paradigm for land use/land cover classification. The Professional Geographer. 60(1), 87.

Platt, R.V., and Goetz A.H. (2004), A Comparison of AVIRIS and Landsat for Land Use Classification at the Urban Fringe. Photogrammetric Engineering & Remote Sensing. 70(7), 813-819.

Priyakant, S., Lalit, K., and Nick, R. (2012). Seasonal Variation in Land-Cover Classification Accuracy in a Diverse Region. Photogrammetric Engineering & Remote Sensing Vol. 78, No. 3, March 2012. 271–280.

Purkis, S.J., Klemas, V.V. (2011). Remote Sensing and Global Environmental Change. John Wiley & Sons. Anderson, J.R., 1976. A Land Use and Land Cover Classification System for Use with Remote Sensor Data. U.S. Government Printing Office.

Richards, J.A., and Jia X. (1999). Remote sensing digital image analysis. Springer, Berlin.

Rodríguez-Galiano, V. F., Ghimire, B., Pardo-Igúzquiza, E., Chica-Olmo, M., & Congalton, R. G. (2012a). Incorporating the downscaled Landsat TM thermal band in landcover classification using Random Forest. Photogrammetric Engineering and Remote Sensing. 78, 129–137

Schriever, J.R., and R.G. Congalton, (1995). Evaluating seasonal variability as an aid to cover type mapping from Landsat Thematic Mapper data in the northeast, Photogrammetric Engineering & Remote Sensing. 61(3), 321–327.

Sendabo, D. (2007). Analysis of Biomass degradation as an indicator of the environmental challenge of Bilate Watershed using GIS techniques, unpublished MSC thesis submitted to Addis Ababa University, Addis Ababa.

Shastri, H., Barik, B., Ghosh, S., Venkataraman, C. & Sadavarte, P. (2017). Flip flop of Day-night and Summer-Winter Surface Urban Heat Island Intensity in India. Sci. Rep. 7, 1–8.

Temesgen, G., Taffa, T., Mekuria, A., & Abeyou, W. (2017). Evaluation and prediction of land use/land cover changes in the Andassa watershed, Blue Nile Basin, Ethiopia. Environmental system research. 15, 10-15.

Wagesho, N., and Goel, M. (2013). Effect of Climate Change on Runoff Generation: An Application to Rift Valley Lakes Basin of Ethiopia. American Society of Civil Engineering (ASCE), Hydrologic Engineering Journal. 18, 1048-1063.

Wagesho, N. (2014). Catchment dynamics and its impact on runoff generation: Coupling watershed modeling and statistical analysis to detect catchment responses. International Journal of Water Resources and Environmental Engineering. 6(2), 73-87, February 2014.

Wolter, P.T., Mladenoff, D.J., Host, G.E., Crow, T.R. (1995). Improved forest classification in the northern Lake States using multi-temporal Landsat imagery. Photogramm. Eng. Remote Sens. 61, 1129–1144.

Xie, Y., Shi, J., Lei, Y., Xing, J. & Yang, A. (2014). Impacts of Land Cover Change on Simulating Precipitation in Beijing Area of China. In 2014IEEE Geoscience and Remote Sensing Symposium. 4145–4148.

Yan, G., Mas, J. F., Maathuis, B. H. P., Xiangmin, Z., & Van Dijk, P. M. (2006). Comparison of pixel-based and object-oriented image classification approaches-A case study in a coal fire area, Wuda, Inner Mongolia, China. International Journal of Remote Sensing. 27, 4039–4055.

Yesuf, H., Assen, M., Melesse, M., Alamirew, T. (2015). Detecting land use/land cover changes in the Lake Hayq (Ethiopia) drainage basin, 1957–2007. Lakes and Reservoirs Research and Management.

Yu, Q., Gong, P., Clinton, N., Biging, G., Kelly, M., & Schirokauer, D. (2006). Object-based detailed vegetation classification with airborne high spatial resolution remote sensing imagery. Photogrammetric Engineering and Remote Sensing. 72(7), 799–811.

Zhuang, X., Engel, B. A., Lozano-Garcia, D. F., Fernandez, R. N., & Johannsen, C. J. (1994). Optimization of training data required for neuro-classification. International Journal of Remote Sensing. 15, 3271−3277.